Kinetics of the barotropic ripple ($P_{\beta'}$)/lamellar liquid crystal (L_α) phase transition in fully hydrated dimyristoylphosphatidylcholine (DMPC) monitored by time-resolved x-ray diffraction

Martin Caffrey, Jacqueline Hogan, and Andrés Mencke
Department of Chemistry, The Ohio State University, Columbus, Ohio 43210-1173 USA

ABSTRACT We present here the first study of the use of a pressure-jump to induce the ripple ($P_{\beta'}$)/lamellar liquid crystal (L_α) phase transition in fully hydrated 1,2-dimyristoyl-*sn*-glycero-3-phosphocholine (DMPC). The transition was monitored by using time-resolved x-ray diffraction (TRXRD). Applying a pressure-jump from atmospheric to 11.3 MPa (1640 psig, 111.6 atm) in 2.5 s induces the L_α to $P_{\beta'}$ phase transition which takes place in two stages. The lamellar repeat spacing initially increases from a value of 66.0 ± 0.1 Å (n = 4) to a maximum value of 70.3 ± 0.8 Å (n = 4) after 10 s and after a further 100–150 s decreases slightly to 68.5 ± 0.3 Å (n = 4). The reverse transition takes place following a pressure jump in 5.5 s from 11.3 MPa to atmospheric pressure. Again, the transition occurs in two stages with the repeat spacing steadily decreasing from an initial value of 68.5 ± 0.3 Å (n = 3) to a minimum value of 66.6 ± 0.3 Å (n = 3) after 50 s and then increasing by ~0.5 Å over a period of 100 s. The transition temperature increases linearly with pressure up to 14.1 MPa in accordance with the Clapeyron relation, giving a dT/dP value of 0.285°C/MPa (28.5°C/kbar) and an associated volume change of 40 μl/g. A dynamic compressibility of 0.13 ± 0.01 Å/MPa has been determined for the L_α phase. This value is compared with the equilibrium compressibilities of bilayer and nonbilayer phases reported in the literature. The results suggest testable mechanisms for the pressure-induced transition involving changes in periodicity, phase hydration, chain order, and orientation. A more complete understanding of the transition mechanism will require improvement in detector spatial resolution and sensitivity, and data on the pressure sensitivity of phase hydration.

INTRODUCTION

Interest in the phase behavior of hydrated phospholipids arises, in part, from their ability to spontaneously aggregate into ordered structures (mesophases) in the presence of water. The phospholipid bilayer is of particular interest because it constitutes the basic structural component of biological membranes. The equilibrium properties of the mesophases formed by phospholipid/water systems have been studied extensively (Luzzati, 1968; Shipley, 1973; Small, 1987; Seddon, 1990; Lindblom and Rilfors, 1989). However, it is only the relatively recent advent of synchrotron radiation and suitable x-ray imaging devices that has enabled time-resolved x-ray diffraction (TRXRD)[1] measurements of transitions between mesophases to be made, thus providing detailed information on the kinetics and mechanisms of these important processes (see Gruner, 1987; Caffrey, 1989*a*,*b*; and Laggner, 1988 for recent reviews).

To date, the majority of TRXRD studies on phospholipid systems have relied on the use of a temperature jump to initiate the phase transition. We present here the results of a kinetic study using pressure jump to trigger the ripple ($P_{\beta'}$)/lamellar liquid crystal (L_α) phase transition in the fully hydrated phospholipid, dimyristoylphosphatidylcholine (DMPC). The use of pressure in kinetic studies of this type offer a number of advantages. For example, unlike temperature jump where conductive heat transfer can be limiting, a pressure jump is rapidly and uniformly transmitted throughout the sample. Further, the pressure perturbation is not considered destructive and is bidirectional, lending itself to cyclic perturbation studies of the type carried out by Johnson et al. (1983).

As a thermodynamic variable pressure is just as important as is temperature. It also has significance in the biological world. For example, marine organisms live under pressures up to 100 MPa.[2] Furthermore, pressure has been shown to reverse anesthesia as well as affecting a host of membrane properties and the rate at which lipid phase transitions occur (Kayama et al., 1979; Wu et

[1]Abbreviations used in this paper: CHESS, Cornell High Energy Synchrotron Source; DEPC, 1,2-dielaidoyl-*sn*-glycero-3-phosphocholine; DHPE, 1,2-dihexadecyl-*sn*-glycero-3-phosphoethanolamine; DMPC, 1,2-dimyristoyl-*sn*-glycero-3-phosphocholine; DOPE, 1,2-dioleoyl-*sn*-glycero-3-phosphoethanolamine; DPPC, 1,2-dipalmitoyl-*sn*-glycero-3-phosphocholine; H_{II}, inverted hexagonal phase; the lipid notation used is that of Luzzati (1968); L_α, lamellar liquid crystalline phase; $L_{\beta'}$, lamellar gel phase; P, pressure; $P_{\beta'}$, ripple or undulated phase; r^2, correlation coefficient;TRXRD, time-resolved x-ray diffraction.

[2]The following units of pressure are provided for the convenience of the reader: 1 atm = 1.013×10^6 dynes/cm^2 = 1.013 bars = 1.013×10^5 N · m^{-2} = 1.013×10^5 Pa = 0.1013 MPa = 14.696 psig = 76 cm Hg (at 0°C) = 760 torr (at 0°C).

0006-3495/91/08/456/11 $2.00

al., 1985; Nagle and Wilkinson, 1982; Yager and Chang, 1983; Chong et al., 1989).

The influence of pressure on the structural properties of model membranes has been extensively studied using techniques such as infrared and Raman spectroscopy (Wong, 1984; Wong and Mantsch, 1988; Wong and Huang, 1989), densitometry (Vennemann et al., 1986), and volumetric measurements (Tosh and Collins, 1986; Johnson et al., 1983). Considerably less work has been carried out using diffraction methods (Stamatoff et al., 1978; Utoh and Takemura, 1985; Braganza and Worcester, 1986; Caffrey and Mencke, 1989; Shyamsunder et al., 1989; Winter et al., 1989; Winter and Pilgrim, 1989).

In the present study, we have used TRXRD to investigate the dynamics and mechanisms of the $P_{\beta'}/L_{\alpha}$ transition in hydrated DMPC. The transition involves quite dramatic changes in the conformational state of the lipid acyl chains from disordered in the L_{α} phase to fully extended and tilted with regard to the bilayer normal in the case of the $P_{\beta'}$ phase. The chain "melting" transition is accompanied by a complete loss of rippling in the lamellae of the $P_{\beta'}$ phase which eventually end up as planar sheets in the L_{α} phase. In the latter phase, bilayer thickness is smaller and the distance separating adjacent bilayers larger than in the $P_{\beta'}$ phase. Further, the surface area occupied by each lipid molecule at the lipid/water interface increases by a factor of 1.13 upon chain melting (Parsegian, 1983). An increase in the volume of the hydrated lipid by a factor of 1.03 has been observed at the $P_{\beta'}$ to L_{α} transition (Nagle and Wilkinson, 1978). Thus, pressure can be used to induce the transition. By suitably controlling sample temperature, we have been able to induce the transition in kinetic experiments with pressures as low as 11.3 MPa in standard quartz x-ray capillaries. This has greatly facilitated kinetic measurements using TRXRD. In this study we find that both the forward and reverse transitions take place in two stages, the first being faster than the second. Further, the transition appears to be reversible and two-state without the accumulation of intermediates, such as nonbilayer structures, in the process.

EXPERIMENTAL PROCEDURES

Materials

DMPC was obtained from Avanti Polar Lipids, Inc. (Birmingham, AL) and was used as purchased without further purification. Water was obtained from a Milli-Q water purification system (Millipore Corp., Bedford, MA).

Sample preparation

Fully hydrated samples of DMPC were prepared for x-ray diffraction by repeatedly vortexing the dry powder in excess (>50 wt%) water above the chain melting transition temperature of 24°C. The thick lipid dispersion was centrifuged into thin-walled (10-μm) quartz capillaries (0.7 mm internal diameter; Charles Supper Co., Natick, MA) using the low-speed setting on a bench top clinical centrifuge (model 1528E; International Equipment Co., Needham Heights, MA).

X-Ray diffraction

(*A*) X-Ray source and camera. Measurements were made using wiggler-enhanced, monochromatic (1.564 Å) focused x-rays on the A1 line at CHESS as previously described (Caffrey, 1987) with the following modifications. A 10-cm long cylindrically bent asymmetric crystal of germanium (111) was used for monochromatization and horizontal focusing. Higher order harmonics were removed and the beam vertically focused by using a 60-cm long platinum- or nickel-coated mirror. Beam size at the collimator was 1.5 mm wide and 0.3 mm high providing 5.1×10^{10} photons/s down a 0.3-mm diam collimator (Charles Supper Co.) with CESR operating at 5.44 GeV and 53 mA total of electron beam current.

X-Radiation damage was minimized by implementing the precautions outlined earlier (Caffrey, 1984, 1987). No one part of the sample was left in the beam for longer than 1 min.

Static and time-resolved x-ray diffraction measurements were made using a home-built, low-angle x-ray diffraction camera with a 0.3-mm diam collimator as described previously (Caffrey, 1987) with the following modification. Instead of lens coupling, the image intensifier was coupled via a reducing fiber optic (Gallileo; Electro-Optics Corp., Sturbridge, MA) to the fiber-optic faceplate on the front surface of a CCD video camera (model 3000F; Fairchild, Milpitas, CA).

(*B*) Static x-ray diffraction. X-Ray sensitive film (DEF5; Kodak, Rochester, NY) was used to record diffraction patterns. Sample temperature was controlled by using a forced-air crystal heating/cooling apparatus (FTS Systems, Inc., Stone Ridge, NY) as previously described (Caffrey, 1987). We estimate temperature stability during a given measurement to be $\sim \pm 0.5$°C. Our accuracy is no better than ±1°C. X-Ray wavelength was determined by using a lead nitrate standard and a carefully measured sample-to-film distance (Caffrey, 1987).

(*C*) Time-resolved x-ray diffraction. The essential components of the system used to make TRXRD measurements include a two-dimensional, live-time x-ray imaging device, a character generator interfaced to a digital voltmeter (thermometer), an electronic clock, a video camera, recorder and monitor, and an image processor. These, along with their performance characteristics, have been described earlier (Caffrey and Bilderback, 1984; Caffrey, 1985; Caffrey, 1987).

Pressure jump

Quartz x-ray capillaries (Charles Supper Co.) of 0.7 mm nominal internal diameter were used as pressure cells. In a given batch of capillaries we chose to work with those having the smallest diameter since these generally withstood the highest pressure. The pressure cell was connected to a commercial argon ($\sim$2,500 psig) cylinder by means of a Teflon liner, vespel ferrules (Alltech, Inc., Deerfield, IL), stainless steel and Flexon tubing, Parker and Swagelock fittings, and hand operated high pressure valves as previously described (Mencke and Caffrey, 1991). Pressure jumps were initiated by adjusting the appropriate hand-operated valves. Temperature was controlled throughout the kinetic measurements by using the forced-air crystal heating/cooling apparatus described above. Air stream temperature was measured using a thermocouple positioned within 1 mm of the capillary and next to the x-ray beam.

Pressure development was not measured simultaneously with the TRXRD measurements. Instead, a pressure gauge was substituted for

the pressure cell and jumps between ambient pressure and 11.7 MPa were recorded on video tape using a video camera directed at the gauge dial. The pressure rise is not instantaneous because the argon gas must flow through a narrow flexon tube and fill the volume of the pressure cell. As the gas overcomes the resistance and flows into the cell, pressure gradually builds, somewhat in analogy with the charging of a capacitor through a large resistor. To obtain a plot of the pressure rise with time an ordinary Bourdon pressure gauge was connected in place of the pressure cell and the moving dial of the gauge was video-taped during the pressure jump. One, thus, obtains the pressure gauge readings as a function of time. To relate this to the case when the pressure cell is connected instead of the gauge, it is necessary to correct for the difference in volumes which are estimated at 2.26 and 1.23 cm^3 for the gauge and the cell, respectively (Mencke and Caffrey, 1991). Since the volume of the cell is smaller than that of the pressure gauge the pressure rise in the cell is a factor of 2.26/1.23 = 1.8 times faster. This pressure rise correction was applied to all pressure jump measurements described in this work (Figs. 3, *E* and *F*). We have assumed that the purely mechanical response time of the pressure gauge, i.e., the flexing of the Bourdon tube and the indicator movement, to be very short and, thus, negligible on the time scale of the pressure jumps.

Data analysis

Our raw data consists of two-dimensional powder diffraction patterns, or parts thereof, recorded in live-time on video tape at the rate of 30 frames/s. Sequential images were digitized using an image processor (Recognition Concepts, Inc., Cedar Rapids, ND) under computer control and patterns were circularly averaged over a 20° arc to increase signal-to-noise ratio. The intensity versus position data was transferred to a Macintosh II computer and the experimentally determined function was fitted by a nonlinear least squares method to the model function

$$f_{\text{fit}}(x, I_\alpha, \mu_\alpha, \sigma_\alpha, I_{\beta'}, \mu_{\beta'}, \sigma_{\beta'}, C) = \frac{I_\alpha}{1 + \left(\frac{x - \mu_\alpha}{\sigma_\alpha}\right)^2} + \frac{I_{\beta'}}{1 + \left(\frac{x - \mu_{\beta'}}{\sigma_{\beta'}}\right)^2} + C,$$

where I, μ, and σ are peak height, radial position, and half-width at half-height, respectively, C is a constant, x is the distance along the radius from the pattern center in Angstroms^{-1} and the indices α and β' refer to the L_α and $P_{\beta'}$ phases, respectively.

It was not possible to use the peak fitting program to analyze the simultaneously recorded low- and wide-angle diffraction data. This was due to the fact that in this particular configuration the low-angle peaks were crowded together and poorly resolved especially during phase coexistence. In this case the radial intensity plots were analyzed by hand to obtain peak position and width data. Peak position was determined by recording the pixel position at the maximum peak intensity and the peak width was taken at half-peak height.

RESULTS

Equilibrium measurements

In the absence of extensive sample cooling fully hydrated DMPC exits in the $L_{\beta'}$ phase below 14°C. With heating, the lipid undergoes a series of thermotropic phase transitions beginning with the so-called pretransition into the $P_{\beta'}$ phase at ~14°C followed by the chain order/disorder transition into the L_α phase at ~24°C (Janiak et al., 1979). This study concerns the latter transition.

The $P_{\beta'}$ phase has a characteristic powder diffraction pattern. In the low-angle region reflections are present in the ratio 1:2:3: . . . (Tardieu et al., 1973; Inoko et al., 1980) which derive from the lamellar repeat spacing. These are accompanied by satellite reflections clustered around the lamellar lines which index according to a two-dimensional oblique lattice. The wide-angle region is dominated by a strong symmetric reflection at 4.2 Å. In contrast, the L_α phase pattern is relatively simple, consisting of a series of low-angle reflections in the spacing ratio 1:2:3: . . . and a diffuse, broad band centered at 4.6 Å. Thus, both regions of the diffraction pattern can be used to monitor progress of the phase transition.

As a preliminary to the kinetic studies, we have carried out equilibrium measurements on fully hydrated DMPC using TRXRD. Low-angle diffraction patterns were recorded at a series of temperatures and pressures. The transition temperature was determined in the heating direction over a pressure range extending from atmospheric pressure to 14.1 MPa. The equation for the line of best fit to five data points is $T = 23.7 + 0.285P$ ($r^2 = 0.959$) when T is expressed in degrees Celsius and P in MPa. From the slope of the line we obtain a measure of the dependence of the $P_{\beta'}/L_\alpha$ transition temperature on pressure, $dT/dP = 0.285$°C/MPa (28.5°C/kbar). Using the Clapeyron relation, $dT/dP = T\Delta V/\Delta H$, we calculate that the volume change, ΔV, at the transition is 40 μl/g when the enthalpy change, ΔH, is 25 kJ/mol (Janiak et al., 1979). The corresponding value determined using dilatometry is 30 μl/g (Nagle and Wilkinson, 1978).

Dynamic measurements

In the course of these studies two types of TRXRD measurements were performed which differed in the angular range covered. In the first case, both low- and wide-angle diffraction data were collected simultaneously in an attempt to correlate in time changes taking place in the long- and short-range order of the underlying structure throughout the barotropic transition. To this end, a short sample-to-detector distance was used and both low- and wide-angle regions of the diffraction pattern were recorded together. Because we were limited by a 40-mm diam active surface on the image intensifier only one-half of the diffraction pattern was actually recorded to maximize angular resolution. Sample patterns recorded for the two limiting phases and in the region of phase coexistence midway through the

pressure-induced transition are shown in Fig. 1. These are presented as one-dimensional intensity (I) vs. radial position corresponding to the scattering angle (2θ) and are referred to as I-2θ scans. Image processing of the powder patterns facilitated radial averaging over 20° to enhance the signal-to-noise ratio. The L_α phase recorded at atmospheric pressure and 25°C shows two well-developed, low-angle lamellar reflections and a broad band in the wide-angle region centered at 4.6 Å (Fig. 1 *A*). At 11.3 MPa, the $P_{\beta'}$ phase again shows two well-developed lamellar reflections with enhanced scattering between and beyond the (001) and (002) reflections which derive from the two-dimensional oblique lattice of the $P_{\beta'}$ phase. The wide-angle region contains a sharp, symmetric reflection at 4.2 Å (Fig. 1 *C*). The region of phase coexistence at 25°C and 11.3 MPa (5.6 s after initiation of the pressure jump) is characterized in the wide-angle region by the presence of a sharp reflection at 4.2 Å and a broad diffuse band at 4.6 Å (Fig. 1 *B*). In the low-angle region coexistence is evidenced primarily by the scattering angle of the lamellar reflections which appear midway between those of the two limiting L_α and $P_{\beta'}$ phases and a pronounced asymmetry in the 001 reflection observed during the early stage of the transition (data not shown) as will be discussed below.

The kinetics of the pressure jump triggered L_α to $P_{\beta'}$ transition was monitored by tracking low-angle peak position and wide-angle peak position and width. The results are presented in Fig. 2. A log-scale time axis is used to facilitate viewing of events simultaneously at

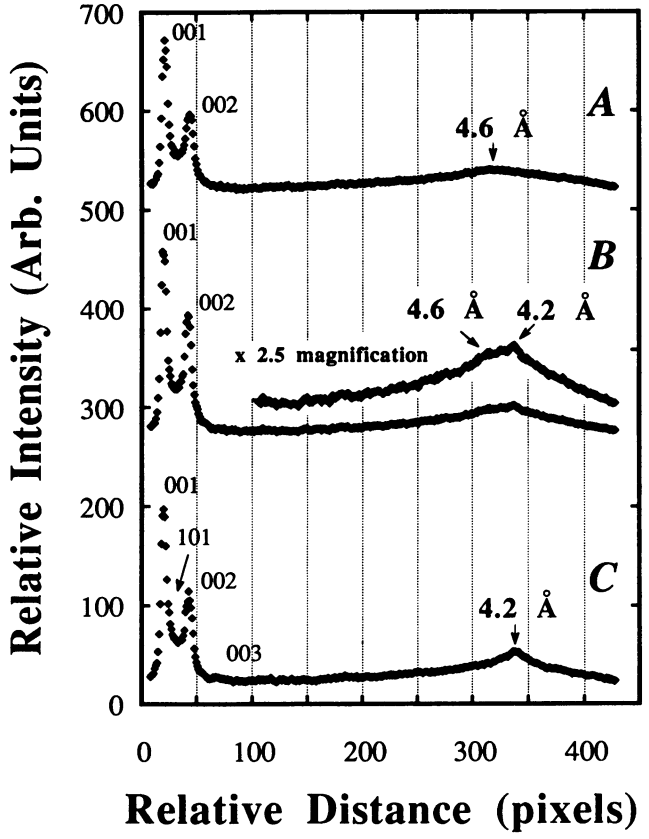

FIGURE 1 Radial averages of the scattered x-ray intensities taken at various times during the pressure-induced L_α to $P_{\beta'}$ phase transition at low- and wide-angles in fully hydrated DMPC at 25°C. (*A*) L_α phase, atmospheric pressure. (*B*) L_α and $P_{\beta'}$ phase coexistence, P = 11.3 MPa, 5.6 s after application of the pressure jump. (*C*) $P_{\beta'}$ phase, P = 11.3 MPa, 3.5 min after application of the pressure jump. The three patterns are displaced on the ordinate for clarity. The wide-angle region of the diffraction pattern could not be calibrated in these experiments, due to nonlinearity of the detector. The arrows at 4.2 and 4.6 Å are provided solely to guide the eye.

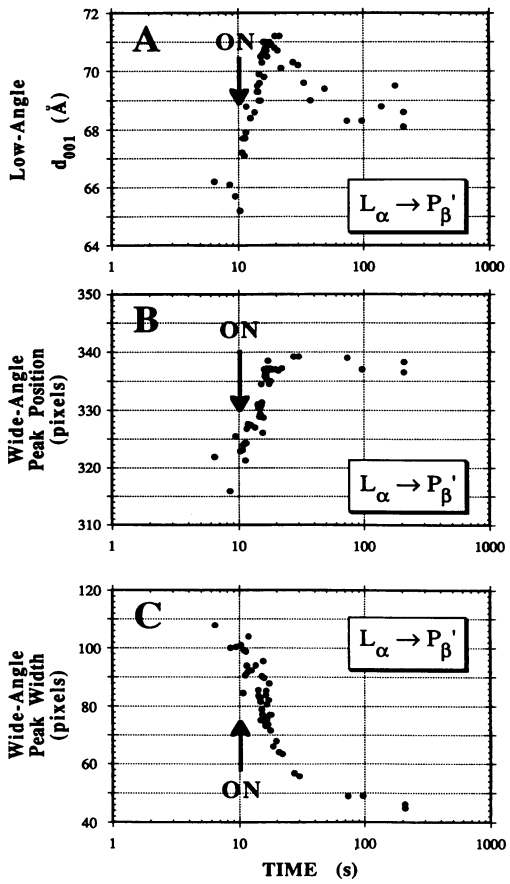

FIGURE 2 Progress of the L_α to $P_{\beta'}$ phase transition in fully hydrated DMPC at 25°C after a pressure jump from atmospheric pressure to 11.3 MPa monitored by using TRXRD. The low- and wide-angle diffraction data were collected simultaneously. (*A*) Position of the low-angle lamellar diffraction peak maximum intensity. (*B*) Position of the wide-angle peak maximum intensity. (*C*) The full-width at half-height of the wide-angle scattering peak. The initiation of the pressure jump at 10 s is indicated by an arrow in each panel.

long and short times after the initiation of the pressure jump at 10 s. Following the pressure jump, dramatic changes take place in both the low- and wide-angle regions of the diffraction pattern. These stabilize after ~100–150 s. In the low-angle region the lamellar repeat d-spacing increases from 66.0 Å in the L_α phase to a maximum of 70.3 ± 0.8 Å ($n = 4$) in ~10 s. The d-spacing then decreases to 68.5 ± 0.3 Å ($n = 4$) over the next 50 s and thereafter remains stable. In contrast, the scattering angle of the wide-angle peak reaches a maximum value within 10 s and remains constant thereafter (Fig. 2 *B*). At the same time, the wide-angle peak width narrows continuously reaching a minimum and limiting value within ~50 s of the triggering event (Fig. 2 *C*). These data suggest that the surface area per molecule in the $P_{\beta'}$ phase remains constant beyond 5–10 s of the pressure jump while the degree of order in the hexagonal chain lattice continues to increase up to 50 s after the jump was initiated.

The wide-angle region of the pattern shows phase coexistence in the region between 14.5 and 17 s as evidenced by the simultaneous presence of the 4.2 Å peak and 4.6 Å band (see Fig. 1 *B*). It is entirely possible that coexistence persists for a longer period than this. However, the sensitivity of the diffraction method to diffuse scatter is low (Caffrey and Feigenson, 1984), and, thus, the exact point in time when the L_α phase finally disappears cannot be established with certainty. The time interval of 2.5 s for phase coexistence is therefore a lower limit.

Evidence for coexisting L_α and $P_{\beta'}$ phases is not readily apparent in the low-angle TRXRD data in the early part of the phase transition, although a pronounced asymmetry in the 001 reflection of the L_α phase is suggestive of same. Further, a continuous change in d-spacing in the time interval of 10–20 s is observed. We suspect this arises because of the limited angular resolution available during these measurements. Thus, the peak position likely reflects the weighted average of the two limiting d-spacing values and the relative amounts of the two phases as the transformation progresses.

The second set of experiments was performed with the sample-to-detector distance considerably lengthened so as to enhance angular resolution in the low-angle region of the diffraction pattern. This was done at the expense of simultaneous low- and wide-angle data collection. The results for both pressurization- and depressurization-induced transitions are shown in Fig. 3. In the pressurization direction we find that, as was observed in Fig. 2 *A*, the lamellar d-spacing rises rapidly from an initial value of 66.0 ± 0.1 Å ($n = 4$) to a maximum value of 70.3 ± 0.8 Å ($n = 4$) within 10 s of the triggering event and then decreases to a stable limiting value of 68.5 ± 0.3 Å over the next 100–130 s (Fig. 3 *A*). Three distinct regions are identified in the progress curves during the pressure-induced transition. In the first second of applying pressure, the d-spacing increases rapidly at a rate ($d_{d_{001}}/dt$) of 1.7 Å/s. During the next 7–8 s, d_{001} continues to increase but at the reduced rate of 0.16 Å/s. After the d-spacing has reached a maximum at ~10 s after the pressurization event, the lamellar repeat decreases at the rate of -9.0×10^{-3} Å/s, reaching an equilibrium value after a further 100–150 s.

In the depressurization direction the lamellar repeat distance decreases from an initial value of 68.5 ± 0.3 Å ($n = 3$) in the $P_{\beta'}$ phase to a minimum value of 66.6 ± 0.3 Å ($n = 3$) in ~50 s followed by a small (0.5 Å) increase over the next 100 s (Fig. 3 *B*). Four distinct regions are identified in this progress curve. The first represents a lag period wherein the $P_{\beta'}$ phase does not respond to the release of pressure. In the next 3 s the d-spacing decreases by ~0.5 Å corresponding to a rate of −0.09 Å/s. During the subsequent 20 s, the lamellar repeat spacing decreases at the rate of ($d_{d_{001}}/dt$) = −0.04 Å/s and reaches a minimum value of 66.6 ± 0.3 Å at ~30 s after depressurization. Following this the lamellar repeat increases at a rate of 2.0×10^{-3} Å/s without limit up to 160 s following the pressure jump.

An expanded version of the early time points in Figs. 3, *A* and *B*, are presented in Figs. 3, *C* and *D*, respectively. The changes in sample pressure with time following the pressurization and depressurization jump are shown in Figs. 3, *E* and *F*. The pressure rise is complete in 1.4 s while the pressure drop is over in 3.6 s (Figs. 3, *E* and *F*). From a comparison of the data in Figs. 3, *C* and *D* with those in Figs. 3, *E* and *F*, it is apparent that regardless of the jump direction pressure has reached its new equilibrium value long before pressure-induced changes in mesophase structure cease. We conclude, therefore, that the transitions are intrinsically slow and are not limited by the pressure jump itself.

Assuming that the L_α phase alone exists in the sample for the first few seconds following the pressure jump (see Discussion) then the initial rise in d-spacing with time (Fig. 3 *C*) reflects the response of L_α phase structure to a rapidly changing ambient pressure (Fig. 3 *E*). The actual initial rate of change in d-spacing is $d_{d_{001}}/dt$ = 1.7 Å/s, while that of pressure is dP/dt = 12.2 MPa/s. Taking the ratio of these two quantities we obtain a measure of the sensitivity of the L_α phase lattice parameter to pressure, namely, $d_{d_{001}}/dP$ = 0.13 ± 0.01 Å/MPa (13 ± 1 Å/kbar). The estimated error of 0.01 Å/MPa arises from not knowing the exact time when the pressure jump was initiated. The 0.5 s lag observed in the response of the L_α phase to the pressure jump (Figs. 3, *C* and *E*) could be due to operator delay in applying pressure or could be an intrinsic property of the L_α phase. The compressibility value of 0.13 ± 0.01 Å/MPa has been calculated consid-

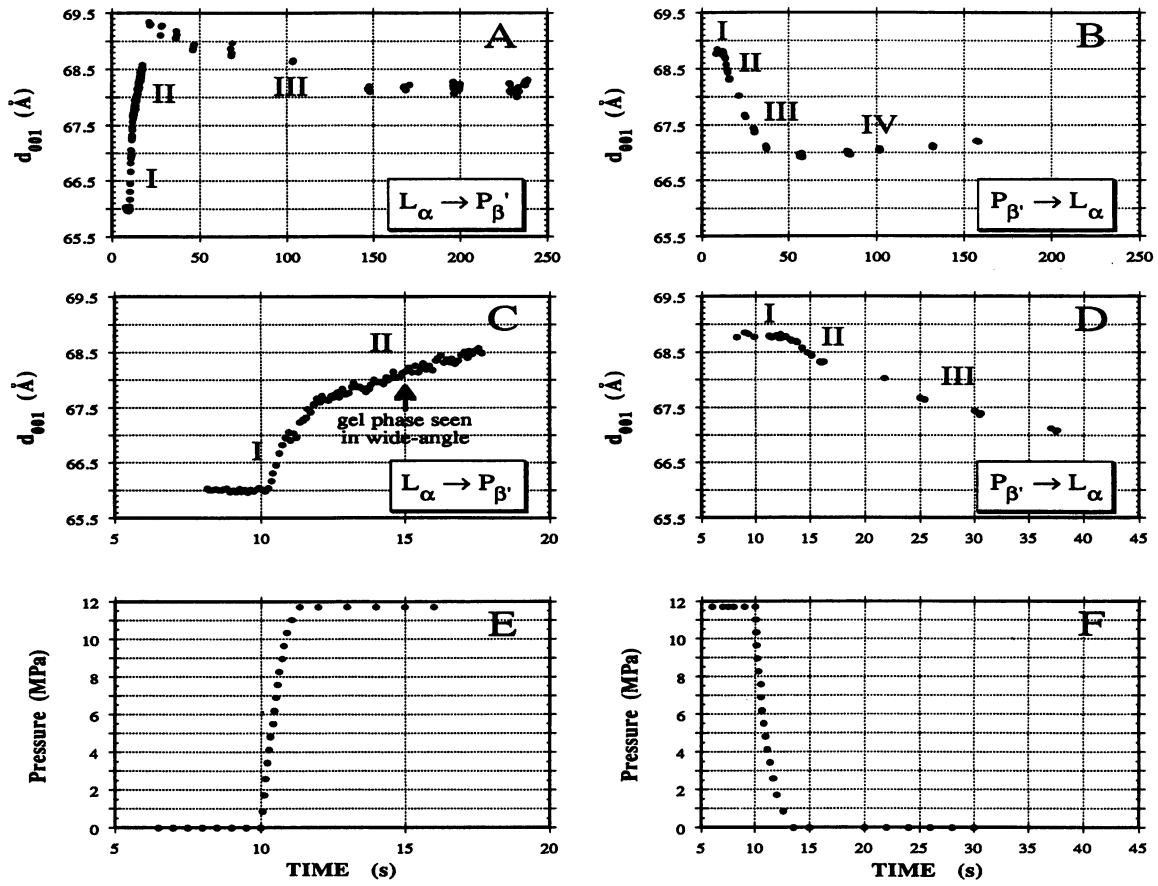

FIGURE 3 Progress of the pressure-induced $P_{\beta'}/L_\alpha$ phase transition in fully hydrated DMPC at 25°C. Changes in the *d*-spacing of the low-angle lamellar diffraction line with time after the application (*A*, *C*) and release (*B*, *D*) of pressure at 10 s (*arrows*) are presented. An expanded view of the early time points in *A* and *B* are shown in *C* and *D*, respectively. The rise and fall of pressure after the application of a pressure jump is presented in *E* and *F*, respectively. As noted under Experimental Procedures, pressure change was measured separately from the collection of TRXRD data.

ering both possibilities. In contrast to the L_α phase, the $P_{\beta'}$ phase structure shows little or no sensitivity to pressure (Figs. 3, *D* and *F*).

DISCUSSION

We have shown that a pressure jump of 11.3 MPa is sufficient to induce the L_α to $P_{\beta'}$ phase transition in fully hydrated DMPC at 25°C. The transition was monitored by TRXRD and measurements were made with the sample contained in a standard thin-walled, quartz x-ray capillary. In the pressurization direction (L_α to $P_{\beta'}$), TRXRD data was collected simultaneously in the low- and wide-angle region. Higher resolution low-angle data was collected in both pressurization and depressurization directions. As will be discussed below, the transition appears to proceed by a two-state mechanism, in the sense that only the $P_{\beta'}$ and L_α phases are observed during the transition. There are no nonlamellar intermediates apparent to within the sensitivity limits of the method.

Pressure dependence of transition temperature

By elevating hydrostatic pressure it is possible to induce a chain disorder to order transition because pressure reduces the cross-sectional area available to the hydrocarbon chain (Braganza and Worcester, 1986). Temperature works in the opposite direction and induces disorder. In the course of this study we determined the dependence of the $P_{\beta'}$ to L_α transition temperature on pressure under equilibrium conditions to be 0.285°C/MPa. This quantity can be interpreted as the decrease in temperature required to bring about the same reduction in fluidity as is produced by a specified pressure in-

crease. The value of 0.285°C/MPa found in this study is in good agreement with previous literature values for synthetic phospholipids with saturated hydrocarbon chains which range from 0.15–0.30°C/MPa (Chong and Weber, 1983; Braganza and Worcester, 1986; Stamatoff et al., 1978).

$P_{\beta'}/L_\alpha$ transition rate and progress curve

We wish to focus on the data presented in Figs. 2 and 3 and to attempt to decipher the progress curves into a defined sequence of events. Events taking place during the thermotropic $P_{\beta'}$ to L_α transition at atmospheric pressure may be described as follows (Cevc and Marsh, 1987). The all-*trans* hydrocarbon chains undergo *trans*-gauche isomerization with concomitant formation of high-density regions within the apolar interior of the bilayer. Internal pressure is relieved by lateral expansion in the bilayer plane which is accompanied by an increase in lipid mobility both in the hydrocarbon region and at the polar/apolar interface. In the process, the more deeply embedded carbonyl oxygens of the acyl chains become exposed, headgroup motion becomes faster, and there is an expansion in the interfacial area per lipid headgroup. The bilayer thins, the ripples disappear, and there is a net uptake of water resulting in an increase in the distance separating adjacent bilayers. A similar set of events of reversed sense takes place upon cooling from the L_α into the $P_{\beta'}$ phase. A particular sequence of events is not implied in the above description.

The progress curves in Figs. 2 and 3 which derive from the pressurization event can be divided into three distinct regions. The first corresponds to the precursor L_α phase responding to applied pressure immediately after triggering. The phase coexistence region makes up the second region, and the third corresponds to the adjustment of the nascent $P_{\beta'}$ phase to the new equilibrium condition. The events taking place in regions one and two are complete within 10–20 s of the triggering event. It is the attainment of the new equilibrium state that is the slowest step in the overall process.

We base our conclusion that the changes observed in lamellar *d*-spacing in the first 1.5 s after the pressure jump are due to the pure L_α phase responding to applied pressure on the following. In this time interval the wide-angle region of the diffraction pattern shows no evidence of gel-phase lipid. Indeed, this gel-phase reflection (at ~4.2 Å) is not seen until 5 s after the initiation of the pressure jump. Further, the equilibrium small-angle neutron scattering measurements of Winter and Pilgrim (1989) show that the lamellar *d*-spacing of the L_α phase in DMPC at 27°C increases by 3 Å upon application of 100 bars (10 MPa) pressure. Despite the differences in temperature, final pressure, and nature of the measurements (dynamic vs. equilibrium) the 1-Å increase observed in our study (Fig. 3 *C*) is certainly not inconsistent with this result.

We also consider the possibility that the changes seen in Figs. 3, *A* and *C* during the first few seconds after the pressure jump arise from the emergence of the $P_{\beta'}$ phase immediately after the triggering event. In this case, failure to detect gel phase in the wide-angle region during this time would have to be ascribed to a poor sensitivity to gel-phase lipid of TRXRD. Further, the continuous increase in *d*-spacing with time would derive from a weighted contribution of the large *d*-spacing characteristic of the $P_{\beta'}$ phase and the smaller but ever increasing L_α lamellar repeat. Such an effect is surely in place during the second stage of the transition in the interval between 12 and 20 s (Figs. 3, *A* and *C*). The slower rise in *d*-spacing here could be attributed to an increase in sample temperature arising from heat liberated during the transition (ΔH = 25 kJ/mol; Janiak et al., 1979) which serves to counter the transition. Heat transfer out of the sample may ultimately dictate the rate of phase transformation.

In the pressurization direction the low-angle region of the diffraction pattern during phase coexistence is cluttered. This derives from the existence of multiple low-angle lamellar reflections characteristic of the $P_{\beta'}$ phase alongside the lamellar reflections of the L_α phase. For this reason the progress curves in Fig. 2 *A* and Figs. 3, *A* and *C* appear continuous as described under Results. The wide-angle data, however, indicate that the transition region is indeed composed of coexisting phases and that the transition is two state in the sense that only two distinct phases exist at any one time during the transition. This result highlights the advantage of recording the TRXRD data simultaneously in the low- and wide-angle region.

The final state of the pressure-induced transition involves a decrease in the lamellar repeat spacing of the $P_{\beta'}$ by 1.5 Å over a period of ~2 min (Figs. 2 and 3). This may be attributed to an increased tilting of the hydrocarbon chains and/or a decrease in water layer thickness as the phase adjusts to the new equilibrium state. The wide-angle data shows that peak position changes little but that peak width continues to decrease during this time period. This suggests that the area per hydrocarbon chain in the $P_{\beta'}$ phase does not change but that the chain lattice becomes more ordered with elapsed time.

While not presented as data under Results, in the course of the TRXRD measurements we noticed an increase in the scattering angle and intensity of the (101) reflection, which arises from the oblique, two-dimen-

sional lattice of the $P_{\beta'}$ phase during the L_α to $P_{\beta'}$ transition. This suggests that the pressure-induced $P_{\beta'}$ phase develops from the L_α phase as long period undulations in a planar precursor, possibly of the type observed by Needham and Evans (1988), whose wavelength shortens with time. In this connection we also note that the (100) ripple repeat has recently been shown to be temperature dependent, decreasing as the main transition is approached (Matuoka et al., 1990). Further insights into this aspect of the transition will require measurements of enhanced angular resolution of the type carried out by Wack and Webb (1988, 1989) and Yao et al. (1991). The development of undulations in planar sheets could account for the slow formation of the ripple phase observed by some workers (Lentz et al., 1978).

The depressurization-induced changes in the diffraction behavior of DMPC at 25°C presented in Fig. 3 *B* have been divided into four stages. We interpret these changes as follows. The first stage in the transformation is a 2–3 s lag wherein no change in the diffraction pattern takes place. Presumably, this reflects the inability of a relatively rigid gel phase with two-dimensional periodicity to respond to pressure. In the next 3 s, the *d*-spacing decreases rapidly by 0.5 Å. This is ascribed to the response of the now, metastable $P_{\beta'}$ phase to the pressure drop and/or to the emergence of the L_α phase whose presence and smaller *d*-spacing will serve to effect a decrease in the measured lamellar repeat. During the next 30 s, the *d*-spacing decreases more slowly to a minimum value of 66.6 ± 0.3 Å ($n = 3$) at ~55 s and most certainly corresponds to the conversion of the sample to the L_α phase. The tardiness of the conversion in this region is likely due, in part at least, to the lowering in sample temperature which accompanies heat uptake, a necessary part of the order-to-disorder transition. The final stage in the transformation involves a slow but steady increase in the *d*-spacing of the nascent L_α phase which continues up to 160 s beyond which no further data were collected (Fig. 3 *A*). It is possible that this *d*-spacing increase corresponds to a relatively slow water imbibition by the L_α phase which, when first formed, is not fully hydrated. In this regard we note that under equilibrium conditions at 1 atm the $P_{\beta'}$ and L_α phases of DMPC saturate at 30 and 40 wt% water, respectively (Janiak et al., 1976, 1979).

Compressibility

Assuming that the phase change does not take place immediately upon application of the pressure-jump perturbation, the data in Figs. 3, *C* and *D*, suggest that the sensitivity of the lamellar *d*-spacing (compressibility)[4] to pressure is considerably greater in the L_α phase ($d_{d_{001}}/dP = 0.13 \pm 0.01$ Å/MPa) than in the $P_{\beta'}$ phase. Unfortunately, we do not have at our disposal the pressure sensitivity of the phase hydration level in the $P_{\beta'}$ and L_α phases. Without this, it is impossible to separate the kinetic compressibility above into lateral and transverse components. Such hydration information is critically needed to fully exploit the structural and mechani-

TABLE 1 Temperature and pressure dependence of the unit cell parameter compressibilities of lipid mesophases

Lipid system*	Phase	*T*	Pressure range	Compressibility‖
		°C	*MPa*	*Å/kPa*
DPMC¶	L_α	27	0–10	300
	L_α	32	0–20	89
	L_α	40	0–40	25
	L_α	40	40–60	40
DPPC/13 wt%**	$L_{\beta'}$	26.5	0–100	−5.4
	L_α	78.5	0–70	27
DPPC/25 wt%‡‡	$L_{\beta'}$	50	110–290	−11
DPPC/D_2O§§	$P_{\beta'}$‡	54.5	50–140	−5
	Lα	54.5	0–350	25
POPC¶	gel	10	70–200	12
	L_α	20	0–100	20
DEPC‖‖	gel	18.6	40–250	20
	L_α	NR§	NR	15
DOPE¶¶	L_α	20	NR	10
	H_I	20	NR	100

*Unless otherwise stated the lipid is considered to be in excess water.
‡See footnote 3.
§Not reported.
‖See footnote 4.
¶Winter and Pilgrim, 1989.
**Stamatoff et al., 1978.
‡‡Utoh and Takemura, 1985.
§§Braganza and Worcester, 1986.
‖‖Winter et al., 1989.
¶¶Shyamsunder et al., 1989.

[3]Although Braganza and Worcester (1986) report that the gel phase is $L_{\beta'}$, the work of Wong et al. (1984, 1985) strongly suggests that the phase below the L_α phase is $P_{\beta'}$. The neutron diffraction exposures of Braganza and Worcester (1986) were of 5 min duration and this, coupled with the observation made during the course of the present work of the slow development of the characteristic ripple reflections, could explain the assignment of an $L_{\beta'}$ rather than a $P_{\beta'}$ phase by these authors.

[4]Compressibility is defined as the change in unit cell parameter (d_{001} for the lamellar phase and d_{10} for the ripple and H_{II} phase) per unit change in pressure. Where data were presented in graphical form, the slope of the best fit line drawn through the data points in the pressure range indicated was taken as the compressibility. Estimated error on these values is ±5%.

cal information contained in the TRXRD data (Parsegian et al., 1979; Cevc and Marsh, 1987).

While the above compressibility data were obtained from kinetic measurements a number of similar studies have been performed under equilibrium conditions and are summarized here for completeness (Table 1). The salient features of the data in the table are as follows. (*a*) The equilibrium measurements oftentimes reveal a nonlinear pressure dependence of phase lattice parameter. For instance, the compressibility of the L_α phase of DMPC at 40°C increased from 25 Å/kPa between 0 and 40 MPa to 40 Å/kPa between 40 and 60 MPa (Winter and Pilgrim, 1989). (*b*) Temperature has a pronounced effect on the compressibility of the L_α phase. For example, in the case of fully hydrated DMPC, the compressibility decreases from 300 to 25 Å/kPA at 27 and 40°C, respectively. The influence of temperature on the compressibility of the other gel and fluid phases has not been established. (*c*) In the case of lipids with saturated acyl chains, the lamellar repeat distance of the gel phases decreases, whilst that of disordered chain phases increases with increasing pressure. However, with lipids containing one or more unsaturated (*cis* or *trans*) acyl chains the lamellar repeat spacing increases with pressure regardless of the state of order of the chains. (*d*) The pressure dependence of the H_{II} phase unit cell parameter in fully hydrated DOPE is 100 Å/kPa. This corresponds to a compressibility some 10 times larger than that of the lamellar repeat in the L_α phase of the same lipid.

Given the sensitivity of the compressibility to temperature and absolute pressure and the limited size of the database in Table 1, a firm statement regarding the relative compressibilities of the different mesophases cannot be made at this juncture. However, the analysis does serve to highlight the need for systemmatic compressibility measurements and for a determination of how the unit cell parameter components, d_w and d_l, vary with pressure. Parenthetically, we note that the dynamic compressibility value of 130 Å/kPa measured for DMPC in the L_α phase is well within the range of values found for this same system under equilibrium conditions.

$P_{\beta'}$ phase metastability and transition reversibility

Recent TRXRD and calorimetric studies have shown that upon cooling from the L_α phase fully hydrated DPPC forms a metastable $P_{\beta'}$ phase, denoted $P_{\beta'}$ (mst) (Tenchov et al., 1989). The original $P_{\beta'}$ and $P_{\beta'}$ (mst) phases differ in that the latter has a higher heat content as evidenced by a lower (by 5%) ΔH for the $P_{\beta'}$ (mst) to L_α transition and has a markedly different low-angle diffraction pattern. While the focus of the present study was on barotropic effects and dynamics, we note that the $P_{\beta'}$ phase observed at 11.3 MPa and 25°C diffracts both at low- and wide-angles analogously to the $P_{\beta'}$ phase obtained upon heating from the $L_{\beta'}$ phase (data not shown). The $P_{\beta'}$ (mst) phase observed by Tenchov et al. (1989) was not seen in the course of the present study. Furthermore, the barotropic transition was found to be reversible with the original L_α phase restored upon pressure release and long-range bilayer correlation was maintained as evidenced by the existence of sharp, well-defined, low-angle diffraction peaks (Fig. 1) throughout the transition. This behavior is in agreement with recent data reported on fully hydrated DMPC (Matuoka et al., 1990).

CONCLUSIONS

Pressure has been successfully used in triggering reversibly the $P_{\beta'}/L_\alpha$ phase transition in fully hydrated DMPC. By suitably adjusting sample temperature, the pressure-jump experiments could be performed in standard x-ray capillaries. The transitions appear to proceed by a two-state mechanism with no nonlamellar intermediates accumulating to within the sensitivity limits of the method. The transition in either the pressure or depressurization direction appears to take place in two steps. The first involves the actual phase conversion itself, which is fast occurring on the time scale of seconds. The second involves a slow relaxation of the new phase toward its final equilibrium state. Dynamic compressibility data indicate that while the $P_{\beta'}$ phase is relatively insensitive to pressure in the range studied, the L_α phase is compressible over a wide pressure range.

Interpretation of the TRXRD data was limited on two counts. Firstly, the angular resolution of the detection/recording device used in this study was such that certain structural details (ripple period and amplitude, *d*-spacings of the individual phases, etc.) of the evolving $P_{\beta'}$ and L_α phases could not be monitored during the transition. Second, the unavailability of data on the pressure sensitivity of phase hydration levels meant that the measured lattice parameters could not be used in phase structure mensuration and in separating total kinetic compressibility into its intra- and interbilayer components. Despite these limitations the present kinetic experiments have enabled us to examine the sequence of events taking place during a rather complex barotropic phase transition which involves changes in chain order and orientation as well as changes in periodicity and phase hydration.

We thank the entire CHESS (National Science Foundation grant DMR12822) and MacCHESS (National Institutes of Health grant RR-014646) staff for their invaluable help and support.

This work was supported by a grant from the National Institutes of Health (DK36849) and a University Exploratory Research Program Award (The Procter & Gamble Co.) and a DuPont Young Faculty Award to Dr. Caffrey.

Received for publication 5 December 1990 and in final form 29 March 1991.

REFERENCES

Braganza, L. F., and D. L. Worcester. 1986. Hydrostatic pressure induces hydrocarbon chain interdigitation in single-component phospholipid bilayers. *Biochemistry.* 25:2591–2596.

Caffrey, M. 1984. X-Radiation damage of hydrated lecithin membranes detected by real-time x-ray diffraction using Wiggler-enhanced synchrotron radiation as the ionizing radiation source. *Nucl. Instrum. Methods.* 222:329–338.

Caffrey, M. 1985. Kinetics and mechanism of the lamellar liquid-crystal and lamellar/inverted hexagonal phase transition in phosphatidylethanolamine: a real-time x-ray diffraction study using synchrotron radiation. *Biochemistry.* 24:4826–4844.

Caffrey, M. 1987. Kinetics and mechanism of transitions involving the lamellar, cubic, inverted hexagonal, and fluid isotropic phases of hydrated monoacylglycerides monitored by time-resolved x-ray diffraction. *Biochemistry,* 26:4826–4844.

Caffrey, M. 1989*a*. The study of lipid phase transition kinetics by time-resolved x-ray diffraction. *Annu. Rev. Biophys. Biophys. Chem.* 18:159–186.

Caffrey, M. 1989*b*. Structural, mesomorphic and time-resolved studies of biological liquid crystals and lipid membranes using synchrotron x-radiation. *Topics in Current Chemistry.* 151:75–109.

Caffrey, M., and D. H. Bilderback. 1984. Kinetics of the main phase transition of hydrated lecithin monitored by real-time x-ray diffraction. *Biophys. J.* 45:627–631.

Caffrey, M., and G. W. Feigenson. 1984. Influence of metal ions on the phase properties of phosphatidic acid in combination with natural and synthetic phosphatidylcholines: an x-ray diffraction study using synchrotron radiation. *Biochemistry.* 23:323–331.

Caffrey, M., and A. Mencke. 1989. Pressure-induced phase transitions in biological liquid crystals: kinetics and mechanism from time-resolved x-ray diffraction. *Biophys. J.* 55:117*a*. (Abstr.)

Cevc, G., and D. M. Marsh. 1987. Phospholipid Bilayers. Physical Principles and Models. Wiley-Interscience, New York. 442.

Chong, P. L.-G., and G. Weber. 1983. Pressure dependence of 1,6-diphenyl-1,3,5-hexatriene fluorescence in single-component phosphatidylcholine liposomes. *Biochemistry.* 22:5544–5550.

Chong, P. L.-G., S. Capes, and P. T. T. Wong. 1989. Effects of hydrostatic pressure on the location of PRODAN in lipid bilayers: a FT-IR study. *Biochemistry.* 28:8358–8363.

Gruner, S. M. 1987. Time-resolved x-ray diffraction of biological materials. *Science (Wash. DC).* 238:305–312.

Inoko, Y., T. Mitsui, K. Ohki, T. Sekiya, and Y. Nozawa. 1980. X-ray and electron microscopic studies on the undulated phase in lipid/water systems. *Phys. Stat. Sol.* 61:115–121.

Janiak, M. J., D. M. Small, and G. G. Shipley. 1976. Nature of the thermal pretransition of synthetic phospholipids: dimyristoyl- and dipalmitoyllecithin. *Biochemistry.* 15:4575–4580.

Janiak, M. J., D. M. Small, and G. G. Shipley. 1979. Temperature and compositional dependence of the structure of hydrated dimyristoyl lecithin. *J. Biol. Chem.* 254:6068–6078.

Johnson, M. L., T. C. Winter, and R. L. Biltonen. 1983. The measurement of the kinetics of lipid phase transitions: a volume-perturbation kinetic calorimeter. *Anal. Biochem.* 128:1–6.

Kayama, H., I. Ueda, P. S. Moore, and H. Eyring. 1979. Antagonism between high pressure and anesthetics in the thermal phase-transition of dipalmitoyl phosphatidylcholine bilayer. *Biochim. Biophys. Acta.* 550:131–137.

Laggner, P. 1988. X-ray studies on biological membranes using synchrotron radiation. *Topics in Current Chemistry.* 145:173–202.

Lentz, B. R., E. Freire, and R. L. Biltonen. 1978. Fluorescence and calorimetric studies of phase transitions in phosphatidylcholine multilayers: kinetics of the pretransition. *Biochemistry.* 17:4475–4480.

Lindblom, G., and L. Rilfors. 1989. Cubic phases and isotropic structures formed by membrane lipids—possible biological relevance. *Biochim. Biophys. Acta.* 988:221–256.

Luzzati, V. 1968. X-ray diffraction studies of lipid-water systems. *In* Biological Membranes. D. Chapman, editor. Academic Press, New York. Vol. 1. 71–123.

Matuoka, S., S. Kato, M. Akiyama, Y. Amemiya, and I. Hatta. 1990. Temperature dependence of the ripple structure in dimyristoylphophatidylcholine studied by synchrotron x-ray small angle diffraction. *Biochim. Biophys. Acta.* 1028:103–109.

Mencke, A. P., and M. Caffrey. 1991. Kinetics and mechanism of the pressure-induced lamellar order/disorder transition in phosphatidylethanolamine: a time-resolved x-ray diffraction study. *Biochemistry.* 30:2453–2463.

Nagle, J. F., and D. A. Wilkinson. 1978. Lecithin bilayers. Density measurements and molecular interactions. *Biophys. J.* 23:159–175.

Nagle, J. F., and D. A. Wilkinson. 1982. Dilatometric studies of the subtransition in dipalmitoylphosphatidylcholine. *Biochemistry.* 21: 3817–3821.

Needham, D., and E. Evans. 1988. Structure and mechanical properties of giant lipid (DMPC) vesicle bilayers from 20°C below to 10°C above the liquid crystal-crystalline phase transition at 24°C. *Biochemistry.* 27:8261–8269.

Parsegian, V. A. 1983. Dimensions of the "intermediate" phase of dipalmitoylphosphatidylcholine. *Biophys. J.* 44:413–415.

Parsegian V. A., N. Fuller, and R. P. Rand, 1979. Measured work of deformation and repulsion of lecithin bilayers. *Proc. Natl. Acad. Sci. USA.* 76:2750–2754.

Seddon, J. M. 1990. Structure of the inverted hexagonal H_{II} phase, and non-lamellar phase transitions of lipids. *Biochim. Biophys. Acta.* 1031:1–69.

Shipley, G. G. 1973. Biological Membranes. D. Chapman, and D. F. H. Wallach, editors. Vol. 2. Academic Press, New York. 1–89.

Shyamsunder, E., P. Botos, and S. M. Gruner. 1989. Comment on: x-ray diffraction study of the effects of pressure on bilayer to nonbilayer lipid membrane phase transitions. *J. Phys. Chem.* 90:1293–1295.

Small, D. M. 1987. Handbook of Lipid Research. The Physical Chemistry of Lipids from Alkanes to Phospholipids. Vol. 4. Plenum, New York. 672.

Stamatoff, J., D. Guillon, L. Powers, and P. Cladis. 1978. X-ray diffraction measurements of dipalmitoylphosphatidylcholine as a function of pressure. *Biochem. Biophys. Res. Commun.* 85:724–728.

Tardieu, A., V. Luzzati, and F. C. Reman. 1973. Structure and polymorphism of the hydrocarbon chains of lipids: a study of lecithin-water phases. *J. Mol. Biol.* 75:711–733.

Tenchov, B. G., H. Yao, and I. Hatta. 1989. Time-resolved x-ray diffraction and calorimetric studies at low scan rates. I. Fully hydrated dipalmitoylphosphatidylcholine (DPPC) and DPPC/water/ethanol phases. *Biophys. J.* 56:1757–1768.

Tosh, R. E., and P. J. Collins. 1986. High pressure volumetric measurements in dipalmitoylphosphatidylcholine bilayers. *Biochim. Biophys. Acta.* 859:10–14.

Utoh, S., and T. Takemura. 1985. Phase transition of lipid multilamellar aqueous suspension under high pressure. II. Structural analyses of lipid bimembrane under high pressure by x-ray studies. *Jpn. J. App. Phys.* 24:1404–1408.

Vennemann, N., M. D. Lechner, T. Henkel, and W. Knoll. 1986. Densitometric characterization of the main phase transition of dimyristoylphosphatidylcholine between 0.1 and 40 MPa. *Ber. Bunsenges. Phys. Chem.* 90:888–891.

Wack, D. C., and W. W. Webb. 1988. Measurements of modulated lamellar $P_{\beta'}$ phases of interacting lipid membranes. *Phys. Rev. Lett.* 61:1210–1213.

Wack, D. C., and W. W. Webb. 1989. Synchrotron x-ray study of the modulated lamellar phase P_{β} in the lecithin-water system. *Phys. Rev. A.* 40:2712–2730.

Winter, R., and W.-C. Pilgrim. 1989. A SANS study of high pressure phase transitions in model·biomembranes. *Ber. Bunsenges. Phys. Chem.* 93:708–717.

Winter, R., C.-L. Xie, J. Jonas, P. Thiyagarajan, and P. T. T. Wong. 1989. High-pressure small-angle neutron scattering (SANS) study of 1,2-dielaidoyl-*sn*-glycero-3-phosphocholine bilayers. *Biochim. Biophys. Acta.* 982:85–88.

Wong, P. T. T. 1984. Raman spectroscopy of thermotropic and high-pressure phases of aqueous phospholipid dispersions. *Annu. Rev. Biophys. Bioeng.* 13:1–24.

Wong, P. T. T., and H. H. Mantsch. 1985. Effects of hydrostatic pressure on the molecular structure and endothermic phase transitions of phosphatidylcholine bilayers: a Raman scattering study. *Biochemistry.* 24:4091–4096.

Wong, P. T. T., and H. H. Mantsch. 1988. Reorientational and conformational ordering processes at elevated pressures in 1,2-dioleoyl phosphatidylcholine. *Biophys. J.* 54:781–790.

Wong, P. T. T., and C.-H. Huang. 1989. Structural aspects of pressure effects on infrared spectra of mixed-chain phosphatidylcholine assemblies in D_2O. *Biochemistry.* 28:1259–1263.

Wu, W-g., L.-G. Chong, and C-h. Huang. 1985. Pressure effect on the rate of crystalline phase formation of L_{α} dipalmitoylphosphatidylcholines in multilamellar dispersions. *Biophys. J.* 47:237–242.

Yager, P., and E. L. Chang. 1983. Destabilization of a lipid non-bilayer phase by high pressure. *Biochim. Biophys. Acta.* 731:491–494.

Yao, H., J. Matuoka, B. Tenchov, and I. Hatta. 1991. Metastable ripple phase of fully hydrated dipalmitoylphosphatidylcholine as studied by small-angle x-ray scattering. *Biophys. J.* In press.